

2-1994

Tunneling into granular Pb films in the superconducting and insulating regimes

Richard P. Barber Jr.

Santa Clara University, rbarber@scu.edu

L. Merchant

Porta Arthur La

Robert C. Dynes

Follow this and additional works at: <http://scholarcommons.scu.edu/physics>



Part of the [Physics Commons](#)

Recommended Citation

R. P. Barber, Jr., L. M. Merchant, A. La Porta, and R. C. Dynes, "Tunneling into granular Pb films in the superconducting and insulating regimes," *Physical Review B*, 49, 3409, (1994).

Tunneling into granular Pb films in the superconducting and insulating regimes

R. P. Barber, Jr., L. M. Merchant, A. La Porta, and R. C. Dynes

Department of Physics, University of California, San Diego, La Jolla, California 92093-0319

(Received 25 October 1993)

Tunneling measurements have been performed on both sides of the insulator-superconductor transition in quench-condensed granular Pb films. The results indicate that the Pb film consists of fully superconducting grains with essentially bulk values for the superconducting energy gap Δ and transition temperature T_c , even when the film exhibits insulating behavior in transport measurements. The density of states inferred from measurements in perpendicular magnetic field are consistent with magnetic spin-flip broadening.

Numerous experiments have been performed to investigate the insulator-superconductor (IS) transition in quench-condensed ultrathin films.¹⁻⁴ In the case of films deposited on clean insulating substrates, an amount of material corresponding to tens of monolayers is required before a measurable electrical conductivity is observed, implying that the morphology of these samples is not uniform, but granular. It is therefore generally agreed that the insulator-superconductor transition is determined by the amount of coupling between individual grains or clusters of grains. On the insulating side of the transition, the resistance of these films increases as temperature is lowered, and below a temperature close to the bulk T_c for the material, the increase becomes faster. This result has been interpreted using a picture where the main transport mechanism is tunneling between the grains. At temperatures where each individual grain becomes superconducting, the change in activation due to the energy gap opening in the density of states of each grain further inhibits transport across the barrier between grains if Josephson coupling is suppressed.¹ As the normal-state resistance of the sample is reduced by incrementally adding material, Josephson coupling between grains improves, and the low-temperature behavior changes from insulating to superconducting with long resistive tails. Small magnetic fields cause large increases in resistance in this regime, due to the field sensitivity of the phase coherence between the grains.⁵

In this paper we report on tunneling measurements into granular Pb films in both the superconducting and insulating regimes. Our results show that the samples have a quasiparticle and gap structure which is indistinguishable from that of a bulk superconductor. Most remarkably, there is no appreciable change in this behavior on the insulating side of the IS transition. This result shows that even though the grains are apparently sufficiently isolated to exclude Josephson tunneling and long-range phase coherence, the individual grains act as bulk superconductors, uncorrelated from grain to grain. Measurements in perpendicular magnetic fields indicate that no normal vortex cores are produced, and the field penetrates more or less uniformly throughout the films with sheet resistances above $10^4 \Omega$. At high fields comparable to H_c for a parallel field, the density of states shows

a broadening consistent with magnetic-field-induced spin-flip scattering. This result also implies that each individual grain is an independent superconductor with a fully developed BCS energy gap.

Fire-polished glass substrates are prepared with thin ($< 100 \text{ \AA}$) Au contact pads and an Al base electrode. The Al contains a small amount of Mn so that it will not superconduct, and a thermally grown oxide layer provides the barrier for the tunnel junction. A layout of the sample geometry is shown in the inset of Fig. 1. The substrate with Al stripe and Au contacts is then mounted to the mixing chamber of a $^3\text{He}/^4\text{He}$ dilution refrigerator to allow for temperature control between 80 mK and 10 K. An evaporation source is mounted opposite the sample in the exchange gas can. A quartz-crystal microbalance is used to monitor the depositions. The entire assembly is immersed in liquid He so that all measurements are performed under ultrahigh vacuum conditions.

The low-temperature granular film deposition is stopped for the first time when the film resistance is in

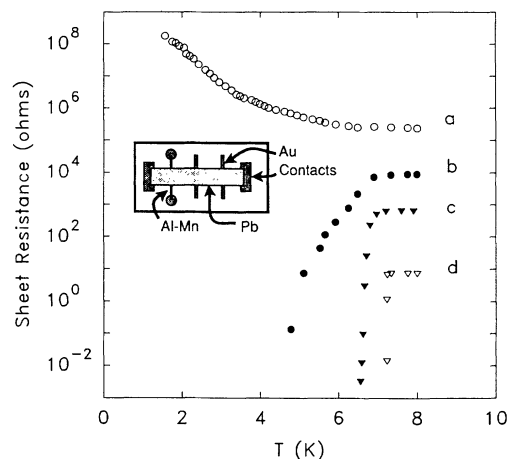


FIG. 1. $R_{\square}(T)$ for four different depositions. Curves (a), (b), and (d) are from the same experimental run and therefore share a common tunnel junction. Inset: Substrate layout for tunneling-transport measurements of quench-condensed films. Au contacts and Al-Mn base electrode are deposited before cooldown. Pb film is evaporated *in situ*.

the range 10^6 – $10^7 \Omega$. This corresponds to a uniform mass thickness of 90–100 Å of Pb. In this regime, resistance depends exponentially on measured thickness. However, previous studies⁵ have shown the samples to have good macroscopic homogeneity in this apparatus. The substrate is held at 10 K to simplify control of the depositions. Sheet resistance versus temperature $R_{\square}(T)$ is measured in addition to the tunneling current-voltage (I - V) characteristics between the Al electrode and the sample at various temperatures. Subsequent incremental depositions of Pb step through the IS transition, and similar data are taken after each deposition. Figure 1 shows representative $R_{\square}(T)$ data for four different depositions. More extensive studies of similar $R_{\square}(T)$ curves have been reported previously.⁵ Curve (a) exhibits apparent insulating behavior ($R \rightarrow \infty$ as $T \rightarrow 0$); curve (b) looks like a superconducting transition with a long resistive tail; and curve (d) is from a thicker film (400 Å) showing a sharp superconducting transition. These three data curves are from the same experimental series and therefore have the same tunnel junction. Only the Pb film thickness is changing. It is interesting to note that for curve (a), $R_{\square}(T)$ shows activated behavior below T_c for Pb, with an activation energy comparable to the superconducting energy gap Δ . For higher sheet resistances, $R_{\square}(T)$ is activated above T_c as well, with a corresponding increase in the activation energy by Δ for $T < T_c$. Curve (c) is from a different series and shows the reproducibility of this experiment. Note that all of these data are plotted as $\log_{10}(R_{\square})$, since there are measurements over nearly 12 orders of magnitude in resistance.

Figure 2 shows the tunneling I - V curves for films *a*, *b*, and *d* at 2.11 K, the lowest temperature at which tunneling into (*a*) is reliable for reasons to be discussed. These curves have been normalized with their respective 8 K (normal-state) tunneling curves. These data are clearly that of superconductor-insulator-normal (SIN) metal tunnel junctions. This result is somewhat remarkable given that the “superconductor” in junction (*a*) is, in fact, a film whose transport measurements indicate it is an insulator.

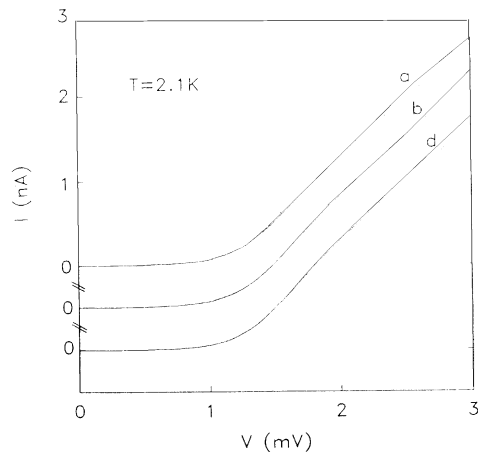


FIG. 2. I - V data from the same tunnel junction for three different depositions (*a*, *b*, and *d* from Fig. 1). Note that there is little difference between tunneling into the superconducting films (*b* and *d*) and the “insulating” one (*a*).

In order for such measurements to be quantitatively meaningful, it is essential to have high resistance junctions so that there is negligible voltage drop across the width of the very high resistance granular film over the sheet defined by the junction. Otherwise, it is not a four-terminal measurement. Typical junction resistances are 10^5 – $10^7 \Omega$. The junction aspect ratio is $\frac{1}{10}$. This geometry allows for tunneling measurements where the film sheet resistance is roughly an order of magnitude greater than the junction resistance. Beyond that point the film is no longer at an equipotential across the width of the junction, and measurements cannot be interpreted assuming the simple tunneling geometry. A more microscopic statement of this criterion is that the tunnel rate of electrons onto the grain must be less than the escape rate of the electrons off the grain. Strictly speaking, there needs to be some conductivity so that it is not a perfect insulator. Hence the measurements must be done at finite T (e.g., $T \geq 2.1$ K), so that there is sufficient leakage to prevent charging effects.

Figure 3 shows the I - V data on the tunnel junction for film (*a*) at various temperatures. Analysis of these data is performed assuming the standard relationship between the superconducting density of states, $N_s(E)$, and the tunneling current for a SIN junction, $I_{ns}(V)$, given by

$$I_{ns}(V) = C_n(V) \int_{-\infty}^{\infty} N_s(E) [f(E) - f(E+V)] dE. \quad (1)$$

Here $C_n(V)$ is the voltage-dependent normal-state conductance and f is the Fermi occupation function at temperature T .⁶ In addition, we have used a more generalized DOS,

$$N_s(E) = \text{Re} \left\{ \frac{E - i\Gamma}{[(E - i\Gamma)^2 - \Delta^2]^{1/2}} \right\}, \quad (2)$$

consisting of the usual BCS result with a broadening

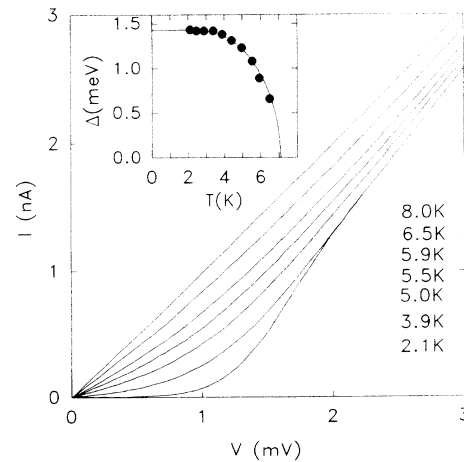


FIG. 3. I - V data for a tunnel junction with an insulating film [curve (*a*) in Fig. 1] at various temperatures. Four traces (between 2.1 and 6.5 K) have been removed for clarity. Inset: $\Delta(T)$ from the fits of tunneling curves in Fig. 3. Note the remarkable agreement with the theoretical curve for Pb (Ref. 9) given that the film is insulating in transport measurements. $\Delta(0)$ is 1.43 meV and T_c is 7.1 K.

term, where Δ is the superconducting energy gap and Γ is a phenomenological broadening parameter.⁷ This type of analysis has typically been performed using conductance data. However, the very large junction and film resistances encountered render standard ac lock-in measurements more difficult. I - V data are therefore analyzed directly using a simplex fitting algorithm.⁸ This program minimizes the difference between the data and the calculated curve by varying one or more parameters in the fit. The quality of this fitting algorithm is demonstrated by its ability to correctly calculate the temperature at which a given I - V curve was taken while T and Δ are both allowed to vary. It is important to point out that the normal-state conductances for all fits are found to be identical, indicating that the changing resistance of the film is not a factor here.

The results of this analysis for film (a) are shown in the inset of Fig. 3 where we plot our fit results for Δ versus T . The lower limit on T is due to the insulating nature of the film as discussed above. As the resistance of the film is increasing exponentially with decreasing temperature, no reliable tunneling data could be taken below this point. The solid line is the calculated $\Delta(T)$ for Pb, a strongly-coupled superconductor.⁹ $\Delta(0)$ is chosen to be the value of $\Delta(1.43$ mV) at the lowest temperature measured (2.1 K). T_c is chosen to be 7.1 K, only slightly depressed from the bulk crystalline value of 7.2 K. Values for Γ in these fits were typically about 50 μ eV except near T_c , where the fitting becomes difficult due to thermal smearing and values up to 100 μ eV were found. These results strongly support a picture in which the films consist of grains with a well-developed superconducting order parameter before the film exhibits long-range phase coherence.

Tunneling measurements were also made with samples in perpendicular applied magnetic field. In a uniform type-II film, the field would produce a vortex lattice. Each vortex will have a normal core. Tunneling measurements can detect the presence of the normal core because the tunneling characteristic in the subgap region will have enhanced conductivity due to normal-normal tunneling. Knowing the applied field, a measure of the area of normal material would allow a direct determination of the size of the vortex cores. In the granular case, the interpretation turns out not to be as simple.

Figure 4 shows the numerical derivative (dI/dV) of the tunneling I - V curve for a film (c) at 0.55 K in a field of 3.3 T. $R_{\square}(T)$ for this film in zero field is shown in Fig. 1. Note that this film has a fairly sharp superconducting transition. These tunneling results, however, suggest that this sample is far from uniform. In fact, not until fields of 1 T or more is there any detectable change in the tunneling characteristics. At this temperature it is a good approximation to use Eq. (1) in the zero-temperature limit, so that dI/dV of the junction is a reasonable measure of the density of states of the sample. The solid line is a fit derived from Skalski *et al.*¹⁰ with a magnetic spin-flip parameter, Γ_m/Δ_0 , equal to 0.07. A similar approach has also been used to calculate the DOS for small superconducting spheres which are smaller than the clean limit coherence length.¹¹ The parameter Γ_m/Δ_0 was found to be equal to $1/2(H/H_c)^2$, where H is the applied field and

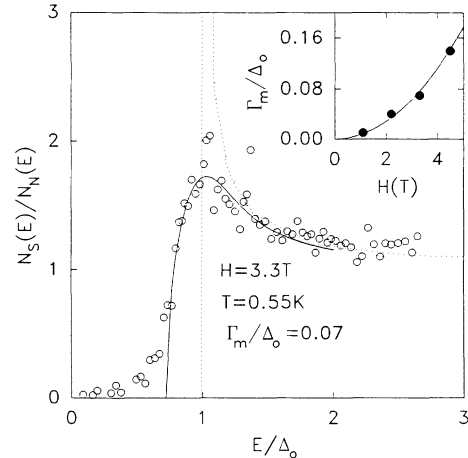


FIG. 4. Normalized derivative of 3.3 T I - V curve along with the density-of-states calculation which includes magnetic spin-flip scattering (solid line) (Ref. 10) and the $T=0$ BCS density of states (dashed line). Inset: Plot of normalized spin-flip parameter vs magnetic field. The solid line is the predicted theoretical dependence given an H_c of 8.4 T (Ref. 11).

H_c is the critical field for the spheres. Correcting Γ_m/Δ_0 to remove the small amount of thermal broadening by subtracting the zero-field value of 0.01, we now plot Γ_m/Δ_0 versus H in the inset of Fig. 4. The solid line is a curve of $\Gamma_m/\Delta_0 = 1/2(H/H_c)^2$ for $H_c = 8.4$ T. This result is in good agreement with measured values of H_c .¹²

The central result of these measurements is the direct observation of the superconducting energy gap on the insulating side of the IS transition. What is perhaps surprising is the fact that the tunneling data change very little across the transition. Values for the broadening parameter, Γ , are only 3–7 % of Δ for film (a) in the temperature range measured. Γ is smaller for films (b) and (d) (0.5–3 % of Δ) but this represents a small difference between curves (a) and (d) in Fig. 2 even though for curve (d) the film is a good superconductor while for (a) it has a sheet resistance of 50 M Ω . These results are in qualitative agreement with previous studies on granular superconducting Sn films which suggested a finite value for Γ which depends on R_{\square} .² From this earlier work on Sn it was expected that Γ would become large (comparable to Δ) for the insulator as the inelastic scattering rate increases, while still going to zero as $T \rightarrow 0$. Such behavior is not observed here even though the Sn results have been reproduced. The values for Γ are considerably smaller for Pb. We are therefore continuing this investigation over a wider parameter space of R_{\square} , T , and grain size. Variations in grain size in the sample should produce variations in Δ , and therefore a larger Γ . Since Sn has smaller grains than Pb, it would be expected that values for Γ would be larger in Sn. The lack of smearing in the Pb tunnel measurements also indicates that there are no substantial inelastic processes occurring in tunneling across the barrier. In terms of sample morphology, these results suggest that the films consist of grains which are large enough to exhibit nearly bulk properties. The small increase in thickness required to change from “insulat-

ing" to superconducting transport is just the amount to cause Josephson coupling between the grains.

The high magnetic fields required to alter the tunneling characteristics in these films is also consistent with this picture. Since the grain or cluster size in these samples is presumably within geometric factors of the critical thickness ($\sim 100 \text{ \AA}$), the magnetic penetration depth is considerably larger. It would therefore be expected that the applied magnetic field penetrates the grains more or less uniformly. There will be no normal vortex cores, and changes will be observable in the DOS due to pair breaking effects. The correct way to think of this is that the field uniformly penetrates the superconductor and there is no appreciable type-II behavior. The value that we extrapolate for H_c , 8.4 T, corresponds to a flux quantum in an area of $2.4 \times 10^{-12} \text{ cm}^2$. This size scale is comparable to the estimated grain size in the sample. For the experimental run from which (c) is taken, the junction resistance was roughly $10^4 \Omega$ while the subgap at 0.55 K was $10^8 \Omega$. We should therefore see additional leakage current when one part in 10^4 of the film has become normal. Using a typical coherence length value of 100 \AA , this would occur at about 1–10 G s in a uniform film. No apprecia-

ble subgap conductance was observed, even at much higher fields. Given the high field tunneling data and the good agreement with predictions of the theory in this regime, the results are roughly what would be expected from measurements on an isolated small superconducting grain. Control of the grain size offers the possibility of a study of the three- to zero-dimensional transition. We are pursuing this possibility.

In summary, we have performed tunneling measurements on granular quench-condensed Pb films on both sides of the insulator-superconductor transition. We conclude that throughout this transition, the individual grains are good superconductors, with near bulk values for T_c and Δ . In high magnetic fields, the tunneling data show no evidence of vortex cores, the magnetic field is uniformly distributed inside the superconductor, and the density of states is broadened due to spin-flip scattering.

We acknowledge fruitful discussions with F. Sharifi, J. Valles, Jr., and J. P. Carbotte. This material is based upon work supported by the National Science Foundation and by ONR Grant No. N00014-91-J-1320.

¹R. C. Dynes, J. P. Garno, and J. M. Rowell, *Phys. Rev. Lett.* **40**, 479 (1978).

²A. E. White, R. C. Dynes, and J. P. Garno, *Phys. Rev. B* **33**, 3549 (1986).

³H. M. Jaeger, D. B. Haviland, B. G. Orr, and A. M. Goldman, *Phys. Rev. B* **40**, 182 (1989), and references therein.

⁴R. Barber, Jr. and R. E. Glover III, *Phys. Rev. B* **42**, 6754 (1990).

⁵R. P. Barber, Jr. and R. C. Dynes, *Phys. Rev. B* **48**, 10 518 (1993).

⁶M. Tinkham, *Introduction to Superconductivity* (McGraw-Hill, New York, 1975), p. 46ff.

⁷R. C. Dynes, V. Narayanamurti, and J. P. Garno, *Phys. Rev. Lett.* **41**, 1509 (1978).

⁸A. La Porta, R. P. Barber, Jr., L. M. Merchant, and R. C. Dynes (unpublished).

⁹J. P. Carbotte (private communication).

¹⁰S. Skalski, O. Betbeder-Matibet, and P. R. Weiss, *Phys. Rev.* **136**, A1500 (1964); and also V. Ambegaokar and A. Griffin, *ibid.* **137**, A1151 (1965).

¹¹S. Strässler and P. Wyder, *Phys. Rev.* **158**, 319 (1967).

¹²J. M. Valles, Jr. and Shih-Ying Hsu, *Phys. Rev. B* **48**, 4164 (1993).

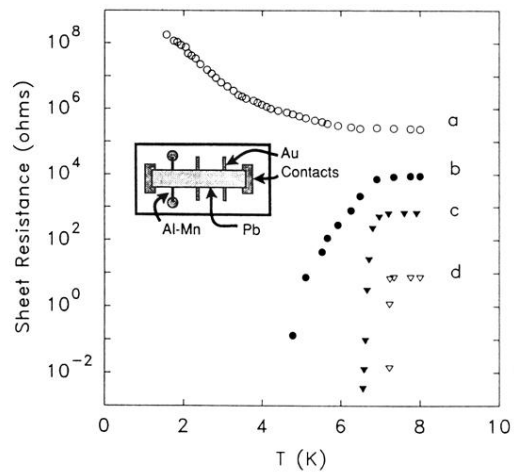


FIG. 1. $R_{\square}(T)$ for four different depositions. Curves (a), (b), and (d) are from the same experimental run and therefore share a common tunnel junction. Inset: Substrate layout for tunneling-transport measurements of quench-condensed films. Au contacts and Al-Mn base electrode are deposited before cooldown. Pb film is evaporated *in situ*.